18th IFHTSE CONGRESS
International Federation for Heat Treatment and Surface Engineering
IFHTSE
ANAIS
PROCEEDINGS
ISSN 1516-392X

EFFECTS OF Si AND Nb ON OXIDATION BEHAVIOR IN HIGH PURITY FERRITIC STAINLESS STEELS[1]

Yasushi Kato[2]
Masatoshi Ito[3]
Osamu Furukimi[3]

Abstract
The effects of Si and Nb on the oxidation behavior at 1073 K in high purity 17Cr steels were investigated in conjunction with the Laves phase. In the early stage of oxidation, mass gains increased not only slightly with Nb addition but also further with the addition of Si and Nb, and precipitation of the Laves phase occurred for a short time with Nb addition and was promoted with Si addition. The increase in mass gain in the early stage of oxidation was seemingly caused by the oxidation of the Laves phase near the surface of steel. The parabolic growth rate constant became small for long-term oxidation with Nb addition in spite of Si addition. The reason for this appeared to be that the Laves phase, which had already precipitated at grain boundaries, suppressed the grain boundary diffusion of cations in steel.
Key words: Stainless steels; Ferritic steels; Oxidation; Laves phases.

[1] *Technical contribution to the 18th IFHTSE Congress - International Federation for Heat Treatment and Surface Engineering, 2010 July 26-30th, Rio de Janeiro, RJ, Brazil.*
[2] *Steel Research Lab., JFE steel corp., 1 kawasaki-cyo cyuo -ku Chiba 260-0836 Japan.*
[3] *Department of Materials Process engineering, Kyusyu Univ. 744 motooka nishi-ku Fukuoka 819-0395 Japan.*

1 INTRODUCTION

The solubility of carbon and nitrogen in ferritic stainless steels, which have a bcc structure, is so low that corrosion resistance tends to decline due to the formation of a Cr-depleted zone along the grain boundaries resulting from precipitation of Cr-carbonitrides at the grain boundaries during heat treatment.[1] Sensitization can be suppressed by addition of Nb, which has greater chemical affinity to C and N than Cr.[2] Nb is also an effective alloying element for enhancing strength at elevated temperatures when in solid solution.[3] Therefore, Nb-bearing ferritic stainless steels have been developed and are mainly used as materials of automotive exhaust parts.

Niobium forms a hexagonal Laves phase of Fe_2Nb at high temperature, and the properties of Nb-bearing ferritic stainless steels are significantly influenced by the precipitation of the Laves phase.[4,5,6] For instance, the high temperature strength of steels decreases as a result of the reduced amount of Nb in solid solution due to the precipitation of the Laves phase.[5] The Laves phase also acts as a notch in the matrix, reducing the toughness of steels.[6]

It is well known that Si is a useful element improving oxidation resistance in ferritic stainless steel, because SiO_2 is more thermodynamically stable than Cr_2O_3 at elevated temperatures.[7] Therefore, an adequate amount of Si has been added to the commercial heat resistant ferritic stainless steels in consideration of its influence on other properties.[8] The standard free energy changes of NbO_2 have an intermediate value between SiO_2 and Cr_2O_3 at elevated temperatures. In recent years, it was found that the addition of Nb and Mo to an 21%Cr-0.1%Si-0.1%Mn-0.1%La steel effectively retards the growth of oxide film while suppressing the grain boundary diffusion of cations by precipitation of the Laves phase at 1073 K.[9,10,11]

In this study, the effects of Si and Nb on the oxidation behavior at 1073 K in 17% Cr ferritic stainless steels in conjunction with the Laves phase (Fe_2Nb) were studied with high purity steels in order to exclude the influence of other alloying elements.

2 MATERIALS AND METHODS

Specimens were melted by high-frequency induction heating in a vacuum and were cast as 30-kg ingots. The chemical compositions of the ingots obtained are shown in Table 1. Impurities in these steels were far lower than those in commercial steels. The ingots were heated at 1443 K for 3.6 ks in an Ar atmosphere and hot-rolled to a thickness of 4 mm, followed by annealing at 1373 K for 60 s in an Ar atmosphere and mechanical de-scaling. These sheets were cold-rolled to a thickness of 1 mm and then degreased. Finally, the sheets were annealed at 1323 K for 60 s in an Ar atmosphere for recrystallization.

Table1 Chemical compositions of specimens studied.

Steel	Cr	Si	Nb	Mn	C	N	S	O	P
	(mass%)				(mass ppm)				
A	17.0	0.005	-	0.01	10	29	7	25	50
B	17.2	0.50	-	0.01	7	28	7	42	60
C	16.9	0.002	0.51	0.01	13	18	7	23	60
D	17.0	0.50	0.50	0.01	13	12	7	11	50

The cold-rolled and annealed sheets were polished with #320 emery paper and subjected to the continuous oxidation test at 1073 K in air for various times. The oxide

films formed during the oxidation tests were investigated by a scanning electron microscope (SEM) with an Energy dispersive X-ray spectroscope (EDX), electron probe micro analyzer (EPMA) and glow discharge spectroscope (GDS). The formed oxide films were identified by the X-ray diffraction spectroscope (XRD). Quantitative analysis of Nb precipitates was performed as described below.[12] The Nb precipitates were totally extracted from the specimens by electrochemical dissolution in a solution of 10 vol% acetylaceton and 1 vol% tetramethylammomium chloride in methanol. The residue was dissolved in a solvent and analyzed by inductive coupled plasma (ICP) measurement. The results corresponded to the total amount of precipitates. Furthermore, the residue was immersed in a solution of 25 vol% sulfuric hydroric acid and then dissolved in a solution of 1 mass% potassium permanganate and 25 vol% sulfuric hydroric acid in order to dissolve only the Laves phase. The residue was dissolved in a solvent and analyzed by ICP measurement. The results were equivalent to the amount of precipitates except Laves phase. Therefore, the amount of the Laves phase in the precipitates was obtained as the difference between the analytical results of this residue and the total amount of precipitates.

3 RESULTS AND DISCUSSION

3.1 Oxidation Test Result

Figure 1 shows the result of the continuous oxidation test. The mass gain of steel B (0.5Si steel) was nearly equal to that of steel A (base steel) until 720-ks oxidation. However, it became smaller than that of steel A for 1440-ks oxidation. In comparison with steel A, steel C (0.5Nb steel) had a slightly larger mass gain for 360-ks oxidation, but a smaller mass gain for 1440-ks oxidation. Although the mass gain of steel D (0.5Si-0.5Nb steel) was more than that of steel A in spite of the oxidation time, the difference in mass gain of both steels became small for 1440-ks oxidation.

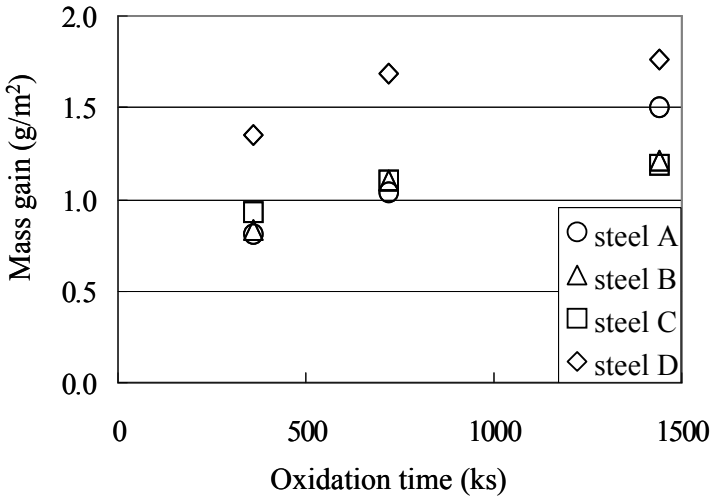

Fig.1 Results of oxidation test.

3.2 Investigation of Oxide Film Formed

Table 2 shows the identification result of oxide films formed with XRD. Cr_2O_3 was detected as a major oxide for all specimens. SiO_2 was weakly detected for steel B and NbO_2 was weakly detected for steel C. Figures 2, 3, 4 and 5 are EPMA results showing the cross-section of each steel after oxidation for 720 ks. In order to protect the oxide film that was formed, the surface of the specimen was covered with an overcoat of evaporated Au and then electrochemically plated with Ni. The oxide films of all steels were mainly composed of Cr and O. Si was discontinuously distributed at the oxide film near to the matrix for steel B. For steel C, Nb was discontinuously distributed at the oxide film near to the matrix. On the other hand, many precipitates were observed inside the matrix for steel C and steel D. These precipitates had a high concentration of Nb for steel C and high concentration of Nb and Si for steel D. These corresponded to the Laves phase, which was precipitated not only at grain boundaries but also within grains during oxidation. It was indicated that formation of oxide film and precipitation of the Laves phase occurred simultaneously in Nb bearing steels.

Table2 Results of identification for oxide layer formed by XRD method.

Steel	360ks	720ks
A	S : Cr_2O_3	S : Cr_2O_3
B	S : Cr_2O_3 W : SiO_2	S : Cr_2O_3 W : SiO_2
C	S : Cr_2O_3 W : NbO2	S : Cr_2O_3 W : NbO2
D	S : Cr_2O_3	S : Cr_2O_3

S:Strongly detected
W:weakly detected

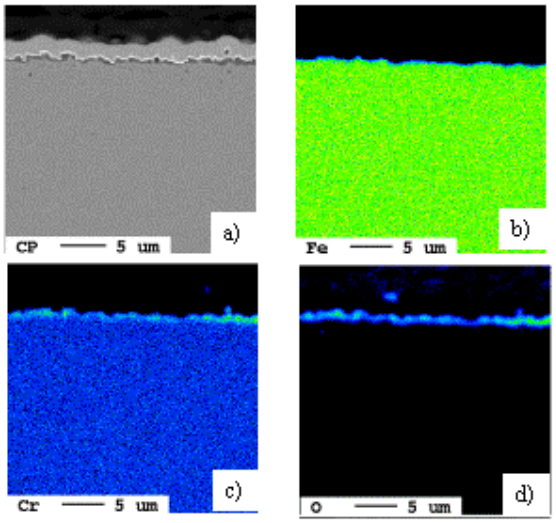

Fig.2 EPMA images of the steel A tested at 1073 K for 720 ks.
a) CP image, b) Fe, C) Cr, d) O

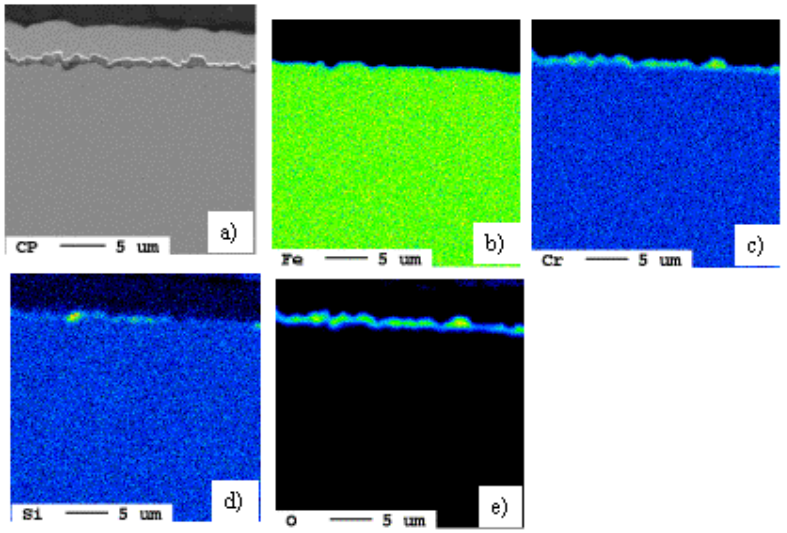

Fig.3 EPMA images of the steel B tested at 1073 K for 720 ks.
a) CP image, b) Fe, c) Cr, d) Si, e) O

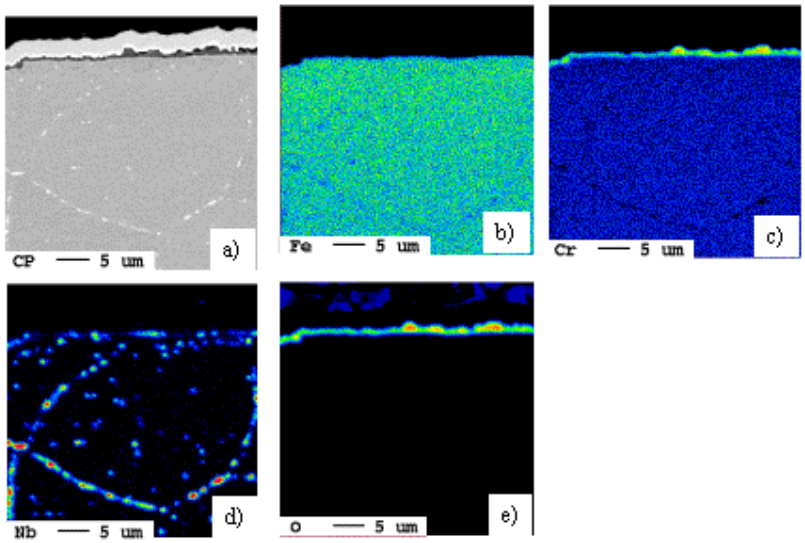

Fig.4 EPMA images of the steel C tested at 1073 K for 720 ks.
a) CP image, b) Fe, c) Cr, d) Nb, e) O

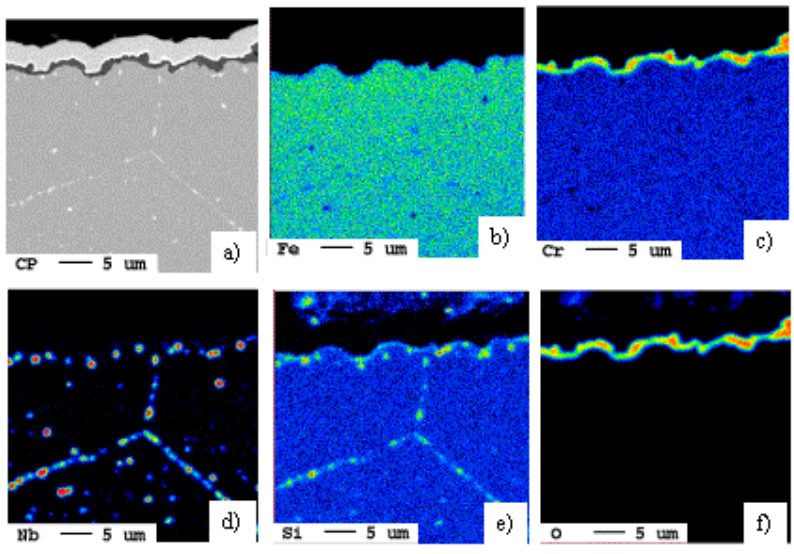

Fig.5 EPMA images of the steel D tested at 1073 K for 720 ks.
a) CP image, b) Fe, c) Cr, d) Nb, e) Si, f) O

3.3 Effect of Laves Phase on Oxidation Behavior

Figure 6 shows changes in the amounts of Fe, Nb and Si as Laves phase for steel C and steel D with heating at 1073 K. In steel C, the amount of the Laves phase increased remarkably after aging for 0.3 ks, and seemingly became constant at 10 ks. On the other hand, in steel D, the amount of the Laves phase increased remarkably after aging for 0.1 ks, and seemingly became constant at 0.9 ks. It was also found that the difference in the amount of Nb as the Laves phase seemed to become constant. Specifically, the amounts of Nb precipitated as the Laves phase was 0.28 mass% in steel C and 0.39 mass% in steel D.

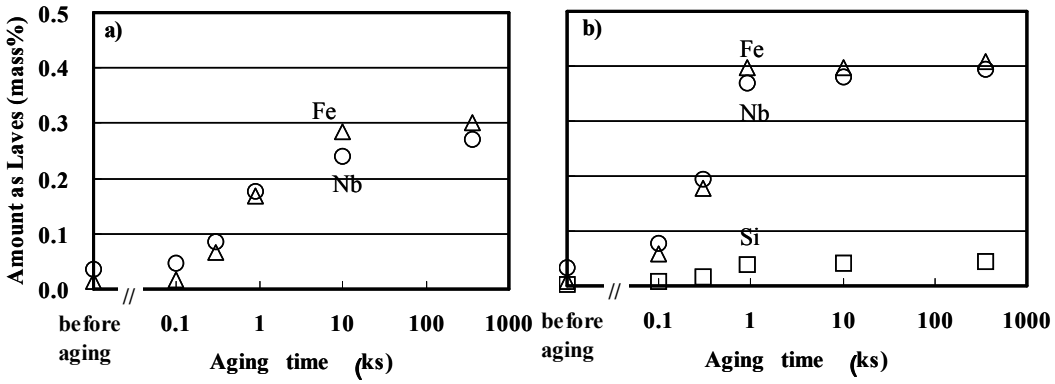

Fig.6 Precipitation behavior of Laves phase at 1073 K. (a):steel C, (b):steel D

The parabolic growth rate constant of oxidation is determined by the following equation:

$$W^2 = k_p t \qquad (1)$$

where W is the mass gain, k_p is the parabolic growth rate constant, and t is the oxidation time. In order to calculate k_p, the relationship between oxidation time and W^2 is shown in Figure 7 for steel A, steel C and steel D. The obtained k_p value was 1.6×10^{-14} $g^2\,cm^{-4}\,s^{-1}$ for steel A. On the other hand, the obtained kp values for the early stage of oxidation were larger than those for long-term oxidation for both Nb bearing steels. The kp values for the early stage oxidation were 2.3×10^{-14} $g^2\,cm^{-4}\,s^{-1}$ and 4.9×10^{-14} $g^2\,cm^{-4}\,s^{-1}$ for steel C and steel D, respectively, while the value for long-term oxidation were 4.5×10^{-15} $g^2\,cm^{-4}\,s^{-1}$ and 3.1×10^{-15} $g^2\,cm^{-4}\,s^{-1}$, respectively. These results indicated that there was a difference in mechanism between the early stage and steady stage of oxidation of steel C and steel D. Figure 8 shows SEM images and EDX analysis results of the specimen surface after oxidation at 1073 K for 0.9 ks. It seemed that oxidation occurred overall, and granular oxides were found to be dispersed. One feature was that the granular oxide in steel C contained Nb as compared with the oxide of the smooth area. Similarly, the granular oxide in steel D contained not only Nb but also Si. We experimentally confirmed that the residues extracted from steel C and steel D, which were mainly composed of the Laves phase, changed to oxides upon heating at 1073 K for 0.9 ks in air. These results suggest that the granular oxide was the oxidized Laves phase.

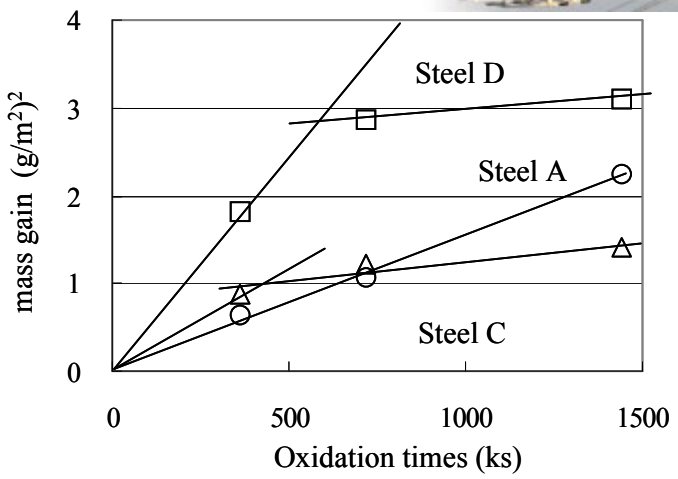

Fig.7 Relationship between W^2 and oxidation time.

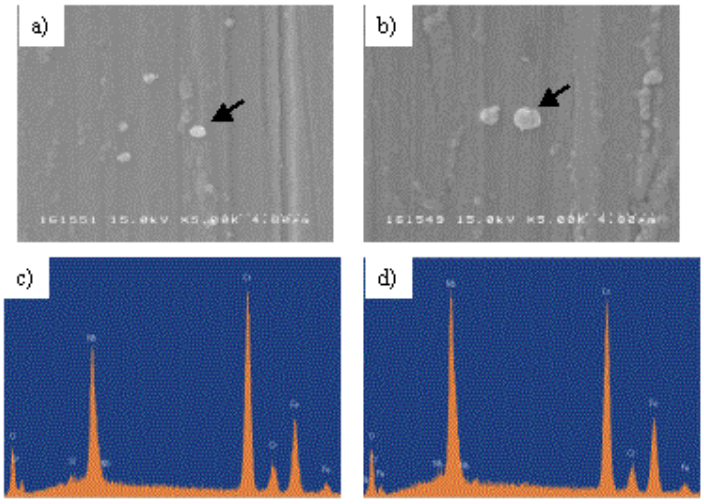

Fig.8. SEM images of sample surfaces after oxidation at 1073 K for 0.9 ks and results of EDS analysis.
a) , c) : Steel C b),d): Steel D

From the above results, the influence of the Laves phase precipitation on an oxidation behavior is discussed below. The Laves phase precipitated for a short time. In the early stage of oxidation, the formation of Cr_2O_3 and the oxidation of the Laves phase on the surface of steel took place simultaneously. Therefore, the mass gain in the early stage of oxidation became large due to the addition of Nb. Furthermore, since the addition of Si not only promoted the precipitation of the Laves phase but also increased the amount of the Laves phase that was precipitated, the mass gain of steel D became larger than that of steel C. After oxidation of the Laves-phase precipitated near to the surface had completed and the surface of the steel was uniformly covered with Cr_2O_3, the oxidation mainly progressed with the growth of Cr2O3. It was thought that the Laves phase, which had already precipitated at grain boundaries, suppressed the grain boundary diffusion of cations in steel, resulting in retardation of the growth of Cr2O3 for long-term oxidation with Nb addition. Therefore, k_p values of both Nb bearing steels became smaller than that of steel A for long-term oxidation. The obtained k_p values of steel C and steel D were close to that of the polycrystalline Cr obtained by Caplan et al. (2×10^{-15} g^2 cm^{-4} s^{-1}).[13]

4 CONCLUSIONS

The effects of Si and Nb on the oxidation behavior of 17% Cr ferritic stainless steels at 1073 K in conjunction with the Laves phase (Fe_2Nb) were studied with high purity steels. The following results were obtained.

1) The major oxide formed was Cr_2O_3 for all steels.

2) In the early stage of oxidation, the mass gain increased not only slightly with Nb addition but also further with the addition of Si and Nb. Precipitation of the Laves phase occurred for a short time with Nb addition and was promoted with Si addition. The increase in mass gain in the early stage of oxidation was seemingly caused by the oxidation of the Laves phase near to the surface of steel.

3) The parabolic growth rate constant became small for long-term oxidation with Nb addition in spite of Si addition. The reason for this appeared to be that the Laves phase, which had already precipitated at grain boundaries, suppressed the grain boundary diffusion of cations in steel.

REFERENCES

1 M.A.Streicher, Corrosion 29 (1973) 337.
2 H.Abo, T.Nakazawa, S.Takamura, M.Onoyama, H.Ogawa, H.Okada, "Stainless Steel '77" Climax Molybdenum Co (1978) 97.
3 N.Fujita, K.Ohmura, M.Kikuchi, T.Suzuki, S.Funaki, I.Hiroshige, Scripta Mater. 35 (1996) 705.
4 A.Miyazaki, K.Takao, O.Furukimi, ISIJ International 42 (2002) 916.
5 N.Fujita, K.Ohmura, A.Yamamoto, Mater. Sci. Eng. A351 (2003) 272.
6 T.Tomita, M.Oku, Nissin Steel Giho 87 (2006) 11.
7 D.Mortimer, W.B.A.Sharp and D.R.Holmes, Proc. 3rd International Conf. on Metallic Corrosion 4 (1969) 382.
8 A.Miyazaki, M.Gunji, K.Yoshioka, Kawasaki Steel Technical Report 31 (1994) 21.
9 S. Ide, Y. Funakawa, Y. Kato, O. Furukimi, Materia Japan 45(2006) 135.
10 S. Ishikawa, S. Ide, Y. Kato, O. Furukimi, Proceedings of the 14th Symposium on Solid Oxide Fuel Cells in Japan Extended Abstract, 2005, 146.
11 S. Ishikawa, S. Ide, Y. Kato, T. Ujiro, Proceedings of the 15th Symposium on Solid Oxide Fuel Cells in Japan Extended Abstract, 2006, 136.
12 M.Inose, K.Fujimoto, Y.Kato, CAMP-ISIJ 20 (2007) 1355.
13 D. Caplan, GI. Sproule, Oxide. Met. 9(1975) 459.